Journal of Cleaner Production 234 (2019) 822–831

Contents lists available at ScienceDirect

Journal of Cleaner Production

journal homepage: www.elsevier.com/locate/jclepro

Investigation of formation mechanism of particulate matter in a laboratory-scale simulated cement kiln co-processing municipal sewage sludge

Zhenzhou Yang [a], Chen Wang [b], Junfeng Wang [c], Lili Liu [a], Xinlei Ge [c, **], Zuotai Zhang [b, *]

[a] Beijing Key Laboratory for Solid Waste Utilization and Management and Department of Energy and Resource Engineering, College of Engineering, Peking University, Beijing, 100871, PR China
[b] School of Environmental Science and Engineering and Key Laboratory of Municipal Solid Waste Recycling Technology and Management of Shenzhen City, Southern University of Science and Technology, Shenzhen, 518055, PR China
[c] Jiangsu Key Laboratory of Atmospheric Environment Monitoring and Pollution Control, Collaborative Innovation Center of Atmosphere Environment and Equipment Technology, School of Environmental Science and Engineering, Nanjing University of Information Science & Technology, Nanjing, 210044, PR China

ARTICLE INFO

Article history:
Received 1 August 2018
Received in revised form
30 May 2019
Accepted 24 June 2019
Available online 25 June 2019

Handling Editor: CT Lee

Keywords:
Waste
Municipal sewage sludge
Cement kiln
Heavy metals

ABSTRACT

The integrated utilization of wastes in a cement kiln has become an international megatrend. Various hazardous compounds containing in wastes might be enriched in the particulate matter (PM) emitted during the waste disposal and cause adverse environmental consequences. In order to evaluate the potential environmental issues caused by the PM emission from the cement kiln for co-processing wastes, the chemical characteristics and formation mechanism of the PM was investigated for the first time by using a laboratory-scale tube furnace to simulate this process. PM was collected to analyze the major components (heavy metals, inorganic and organic components) and morphologies. The results reveal that volatile heavy metals in municipal sewage sludge (MSS) can be enriched in PM. The process can elevate the levels of sulfate and the organic contents in PM, and the existence of organic moieties such as CN^+ and CHN^+ suggest that the co-processing of MSS can affect the PM organic compositions. Single particle imaging analyses indicate that PM can be classified into nine types based on their elemental compositions. Further analysis reveals that most particles usually mix with other types of particles and those mixed particles may cause a more serious impact on the environment. Based on the TEM observation, a two-step formation mechanism of PM is proposed. Our findings point out the potential environmental adverse effects and call attentions to a full environment assessment of this new type of cement production process, and also indicates stringent measures should be taken to reduce PM emissions during this process.

1. Introduction

Municipal sewage sludge (MSS) is a common waste worldwide, and its production has reached 30 Mt/y with an annual increasing rate of 8–10% (Xiao et al., 2017). The accumulation of MSS has become a serious environmental concern. Landfill and incineration are the two most common routes for MSS disposal in China (Zhou et al., 2014). Such methods have their own bottlenecks. For example, the reduction of land resource and undesired emissions (e.g., leachate and landfill gas) to ambient water, soil and air restricts the implementation of landfills (Jin et al., 2017). Incineration can also aggravate emissions of hazardous substances such as heavy metals and some organic species into the environment. The methods of gasification, pyrolysis and digestion have been proposed for the disposal of MSS, but the associated intensive energy consumption, complex operation, etc., may also limit further development of those methods. The integrated utilization of wastes such as MSS in cement kiln has become a promising method and attracts public interests due to its multiple advantages. For example, the MSS contains Ca, Si and Al, which are similar to the raw materials for cement production and the co-processing of MSS

* Corresponding author.
** Corresponding author.
E-mail addresses: caxinra@163.com (X. Ge), zhangzt@sustc.edu.cn (Z. Zhang).

https://doi.org/10.1016/j.jclepro.2019.06.280
0959-6526/

in a cement kiln can save natural resources. Dried MSS also contains significant calorific values, which could save energy at the same time. The silicate in the cement clinker such as tricalcium silicate and dicalcium silicate can help stabilize the heavy metals during the high temperature calcination process. Hazardous organic substances might also be decomposed due to the high temperature and long residence time in a cement kiln. The co-processing of wastes in cement kiln can also receive subsidies from the government. Despite aforementioned advantages, this disposal method may pose some environmental problems, such as the emission of particulate matter (PM) into the air.

It is well known that PM has significant effects on human health, ecosystems and the climate (Huang et al., 2014). For example, haze pollution events caused by the high concentration of PM frequently occur in China (Sun et al., 2015). The integrated utilization of MSS in cement kilns has been widely implemented all around the world. Comparing to regular fuel, higher contents of heavy metals and organics are contained in MSS. During the high-temperature calcination process, a portion of those hazardous substances can be decomposed or be immobilized in the cement clinker, while the remaining portion might be evaporated in a gas phase. Those pollutants in a gas phase can be condensed on the surface of PM and be released into the air, posing a threat to the environment and human health (Schuhmacher et al., 2009).

A number of research efforts have been conducted on the airborne pollutants including heavy metals (Yang et al., 2016), NO_x (Jeschar et al., 1999), SO_2 (Asamany et al., 2017) and organics (Jin et al., 2016). Very few studies focused on the secondary PM in the air nearby the cement plant by using the atmospheric chemistry methods (Yang et al., 2018). These authors conducted a field study in a cement plant co-processing hazardous wastes. The various anthropogenic and natural activities nearby the cement plant, such as vehicle emissions can affect and complicate analyses of the physiochemical properties of ambient PM (Zhao et al., 2018), it was difficult to identify the sole influence of the wastes on the properties of PM. To achieve a better understanding of the impact of wastes on the physiochemical properties of primary PM emitted from the cement kiln and their formation mechanism, in the present work, PM samples were collected from the emissions out of the laboratory-simulated process. The chemical properties of water-soluble organic matter (WSOM) in the emitted PM was probed by using the Aerodyne high-resolution soot-particle aerosol mass spectrometer (SP-AMS). The formation mechanism of the mixing state of PM was discussed with the help of a single particle analysis method. Cement production is one of the most important industrial activities that can release PM into the environment, accounting for 40% of total industrial PM emissions in China. Due to the multiple advantages, the co-processing of wastes in cement kiln has been widely implemented around the world, therefore the PM emitted such process should be investigated as well. Our study focuses on the PM properties and its formation mechanism from a simulated cement kiln co-processing of wastes. Our results are expected to provide useful insights to the environmental assessment, pollution reduction when such a technology is implemented and is beneficial to the goal of cleaner production.

2. Materials and methods

2.1. Raw materials and sample collection

In this work, the calcined raw materials were PO 42.5 (strength class 42.5 in the standard GB 175–2007) cement raw meal, coal and municipal sewage sludge (MSS), which were provided by a cement plant located in Beijing. Cement raw meal includes limestone, fly ash, sandstone and iron powder, which can be used to produce cement clinker. Coal is added to simulate the fuel in a cement kiln, and MSS is the waste to be disposed. In the experiment, the cement raw meal was in a fixed proportion (85 wt%), while the rest was made up of mixtures of coal and MSS. A replacement of 15 wt% MSS is indeed used in a real process. We then designed a series of experiments (Samples 1 to 6) with the coal fractions varying from 15 wt% to 0 wt%, and the corresponding MSS fractions from 0 wt% to 15 wt%. The sample name and corresponding compositions are shown in Table S1 in the supplementary information (SI). These raw materials collected from the cement plant were fully blended by a ball mill (QM-3SP2, Tincan, China) for 24 h, and then were fed into the furnace for calcination. Note here the samples were prepared on a mass basis, while in real process, by considering the different calorific values between the coal and MSS, replacement based on an energy-basis is preferred.

The chemical compositions and mineralogy of raw materials can be determined by an X-ray fluorescence spectrometer (XRF, S4-Explorer, Bruker, US) and an X-ray diffraction (XRD, D/MAX-PC 2500, Rigaku, US), respectively. The major components of raw materials are presented in Table 1. It can be seen that the cement raw meal for the cement production is composed mainly of SiO_2, CaO, Fe_2O_3 and Al_2O_3. The content of phosphorus oxide in the MSS is also high, which can be attributed to the lack of a phosphate elimination process in the wastewater treatment plant (Folgueras et al., 2004). Fig. 1 shows the XRD patterns of raw materials. It can be seen that the crystalline phases of SiO_2, $CaCO_3$ and Fe_2O_3 are identified in cement raw meal. This outcome can be attributed to the fact that the cement raw meal is composed of sandstone, limestone, iron ore and fly ash. The major components of coal are SiO_2 and $Al_2Si_2O_5(OH)_4$, while $Ca_3(PO_4)_2$ and SiO_2 are identified in MSS. The contents of heavy metals in raw materials are also shown in Table 1. Compared to cement raw meal and coal, heavy metal concentrations in MSS are notably high.

The equipment used for raw materials calcination was a laboratory-scale electrically heated tube furnace (F1600, Zhonghuan, China). The samples were calcined according to the programmed procedure. The temperature was raised at the rate of 10 °C/min from room temperature to 950 °C, and maintained for 30 min, then the temperature was increased to 1450 °C at a rate of 10 °C/min and held for 2 h, which is similar with the temperature program during the real cement production process. During the practical cement production process, raw materials are firstly fed into the pre-calciner for the full decomposition of limestone, where the temperature is about 950 °C. Then the raw materials are transferred to the rotary kiln for the cement clinker calcination, where the temperature is about 1450 °C. The 6 p.m. samples were collected in the nozzle of the furnace by quartz filters (9 cm, QMA, Whatman, UK) with an air flow rate of 1.2 L/min during the entire calcination process. The air flow rate in the laboratory study is also similar with that in the real cement production process.

2.2. Sample analyses

The overall diagram of sample analyzing procedure is shown in Fig. S1. Before the heavy metal measurement, approximately 1/4 of the quartz filter was pre-treated in a microwave digestion system. The digested solution was subsequently sent to an inductively coupled plasma mass spectrometer (ICP-MS, XSERIES 2, Thermo Scientific, US) for heavy metals (As, Ni, Cd, V, Cr, Mn, Ba, Sr, Cu, Zn and Pb) analysis. The concentrations of heavy metals in the flue gas can be calculated according to Eq. (1). In Eq. (1), C refers to the concentration; V reveals the volume; M represents the mass; S is the flow rate; T stands for time. Specifically, C_1 (μg/mL) is the concentrations of heavy metals in extracted solution and V_1 (mL) is the volume of solution used to dissolve the filter; M_t (g) is the total

Table 1
Main chemical com positions (wt%) and concentration of heavy metals of cement raw meal, sewage sludge (MSS) and coal (mg/kg).

Sample	CaO	SO_3	SiO_2	MgO	Al_2O_3	Na_2O	Fe_2O_3	K_2O	P_2O_5	LOI
Cement raw meal	46.9	0.1	9.0	1.8	3.8	0.1	1.7	0.6	0.1	35.1
Coal	2.3	0.3	4.4	0.1	2.0	0.1	1.5	0.2	0.1	89.1
MSS	7.6	1.4	14.2	2.3	7.8	0.9	4.1	1.4	7.2	51.0

	As	Sr	Ba	Cd	Co	Cr	Cu	Ni	Pb	Zn	Mn	V	Sn
Cement raw meal	134	381	54	Nd	3	295	16	7	17	46	268	13	31
Coal	126	467	358	1	3	322	16	9	4	39	77	14	36
MSS	196	424	525	Nd	6	438	276	28	37	800	401	21	34

Nd: not detected; LOI: Loss on ignition; refers to the sample heated to 800 °C for 3 h using American Public Health Association (APHA) standard method.

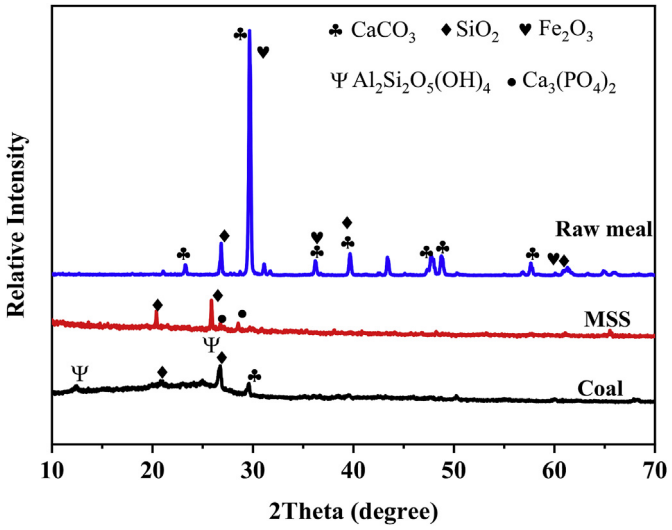

Fig. 1. The XRD patterns of raw materials.

mass of the filter; S_2 is the gas flow rate (m^3/min); while T_2 is the experimental time (min), and M_1 (g) is the mass of 1/4 of the filter used for the heavy metals measurement. The enrichment factors (EFs) of heavy metals can be determined by Eq. (2) (Yang et al., 2018): EF_i refers to the EFs; X_i reveals specific element while T_i is the reference element. Sr is the reference element because it can be used to represent natural background aerosols (Dongarrà et al., 2007).

$$C = \frac{C_1 \times V_1 \times M_t}{S_2 \times T_2 \times M_1} \quad (1)$$

$$EF_i = \frac{(X_i/T_i)sample}{(X_i/T_i)crust} \quad (2)$$

Another 1/4 of the filter was sonicated in 40 mL of ultrapure water (18 ± 1 M Ω cm^{-1}) for 30 min under the temperature of 0 °C. Then the extracted solution was filtered through a microporous membrane with a 0.45-μm diameter. Part of the solution was sent to ion chromatograph (IC, CS-2500, DIONEX, US) for the detection of inorganic ions (SO2- 4, NO- 3, Cl^-, F^-, PO3- 4, Na^+, Mg^{2+}, K^+, Ca^{2+} and NH+ 4). Detailed operation parameters have earlier been illustrated by Yang et al. (2018). The details of quality control for the ICP-MS and IC measurements are provided in the supplement SI, and the samples were run in triplicate to check the reproducibility. Then the molar equivalent of cations and anions could be determined by Eq. (3) and (**4**) (Yang et al., 2018); the molar ratio of [NH+ 4] to [SO2− 4] could be defined in Eq. (5) and the equivalent molar ratios (microequivalents) of measured NH+ 4to the sum of NO− 3and SO2− 4 can also be calculated as Eqs. (6)-(7) (Wang et al., 2016a).

$$\sum Cation = \frac{M[Na^+]}{23} + \frac{M[NH_4^+]}{18} + \frac{M[K^+]}{39} + \frac{M[Mg^{2+}]}{12} + \frac{M[Ca^{2+}]}{20} \quad (3)$$

$$\sum Anion = \frac{M[Cl^-]}{35.5} + \frac{M[F^-]}{19} + \frac{M[PO_4^{3-}]}{31.7} + \frac{M[NO_3^-]}{62} + \frac{M[SO_4^{2-}]}{48} \quad (4)$$

$$[NH_4^+] \Big/ [SO_4^{2-}] = (M[NH_4^+] \Big/ 18) \Big/ (M[SO_4^{2-}] \Big/ 96) \quad (5)$$

$$M[NO_3^-] + M[SO_4^{2-}]microequivalents = M[SO_4^{2-}] \Big/ 48 + M[NO_3^-] \Big/ 62 \quad (6)$$

$$M[NH_4^+]microequivalents = M[NH_4^+] \Big/ 18 \quad (7)$$

An SP-AMS was introduced for the WSOM analysis in the PM (Ge et al., 2017). The liquid samples extracted from the PM were nebulized by an atomizer, then were transferred to SP-AMS, and the information of the non-refractory species was ascertained by a high-resolution time-of-flight mass spectrometer based on the mass-to-charge (m/z) ratios. The blank filter was also pretreated and analyzed using the same method as the samples. The measurement was conducted twice for the repeatability, and the detailed operation conditions were similar to the previous studies (Ge et al., 2014). The mass spectra of WSOM, hydrogen-to-carbon (H/C), nitrogen-to-carbon (N/C) ratios, oxygen-to-carbon (O/C) and organic mass-to-organic carbon (OM/OC) ratios were determined by SP-AMS, according to the procedure introduced by Aiken et al. (2008). The particles in filters were ultrasonically dispersed in alcohol, then were adhered on the Cu-film. The morphology and elemental compositions of an individual particle was analyzed by transmission electron microscopy (TEM, F20, Tecnai, US) equipped with energy-dispersive X-ray spectrometer (EDS, F20, Tecnai, US). The TEM observation started from the center and fanned out to the edge of the film to ensure that the analyzed particles are representative (Yang et al., 2018).

3. Result and discussion

3.1. Characterization of heavy metals in PM

To better understand the characteristics of heavy metals emitted during the cement clinker calcination process, thermodynamic equilibrium calculations were conducted using FactSage 6.4 (Becidan et al., 2010). The input data are based on the chemical

compositions of feeding materials and the real air conditions. The temperature is in the range of 700–1500 °C. Although the equilibrium calculation contains the limitation because it ignores the kinetic behaviour, it can help to explore the volatilization behaviours of heavy metals under various conditions. The results are shown in Fig. S2. The heavy metals can be classified into three categories under the cement calcination conditions: the most volatile elements are Cd, As, Zn and Pb; Ni, Cu, Cr and Ba are considered semi-volatile elements; and V and Mn can be treated as non-volatile element. The concentrations of heavy metals in flue gas are shown in Fig. 2. As can be seen in this figure, Zn, Cr, As and Ba show high concentrations, which can be attributed to the high contents of those elements in the raw materials (Table 1). Although Mn also shows high content in the raw materials, its concentration in the collected PM is low because of its low volatility. The EFs for various heavy metals were also calculated. An EF value less than 10 indicates that the cement production process does not affect the distribution of heavy metals in the ambient PM. The EF larger than 10 indicates the cement production can elevate the heavy metals concentrations in the PM.

The estimated EFs for all heavy metals are given in Table 2. It can be seen that all heavy metals have larger EFs compared to the background values in Beijing (Gao et al., 2014), indicating that the cement production process could facilitate the enrichment of heavy metals in PM. Most heavy metals become more enriched in the PM with increasing amounts of MSS. This outcome might be because the MSS contains much higher contents of heavy metals than those present in the coal used (Table 1), elevating the heavy metals contents in the PM. Since MSS often contains a higher content of chlorine than the raw materials, the reaction with heavy metals results in forming the highly evaporable chloride (Li, 2013). The addition of MSS can also facilitate the volatilizations of heavy metals during the cement clinker calcination process. The EFs of Cd, Pb, V and Mn increase first then decrease with further additions of MSS. The reason for this outcome might be that MSS also contains higher content of SiO_2 and CaO than that in coal, and some heavy metals can react with SiO_2 and CaO in MSS to form the stable species during the calcination process. For example, Cd and Pb can react with SiO_2 to form $CdSiO_3$ and $PbSiO_3$, while V can react with CaO to form $(CaO)_2(V_2O_5)$. These are confirmed by the thermodynamic equilibrium calculations (Fig. S2), indicating that the EFs of some heavy metals do not always increase with further additions of MSS.

Table 2
The EFs of heavy metals in particulate matter.

Sample Name	Ni	Cd	V	As	Pb	Zn	Cu	Cr	Ba	Mn
1	14.1	322	3.0	1375	12.0	59.8	24.5	310	11.8	0.38
2	13.8	512	2.4	1480	11.5	77.8	32.5	286	11.5	0.50
3	14.7	515	2.7	1440	20.5	77.7	31.3	295	11.0	0.42
4	16.5	1514	3.8	1625	19.4	69.5	30.2	311	10.0	0.78
5	17.2	2200	4.3	1720	26.2	70.5	35.5	305	12.0	1.18
6	16.3	1050	2.9	1825	11.1	82.5	39.4	341	13.8	0.44

3.2. Characterization of water-soluble inorganic ions in PM

The concentrations of the water-soluble inorganic ions and their relative mass proportions are shown in Fig. 3. The hierarchy of their concentrations is as follows: SO2- 4 > NH+ 4 > Ca^{2+}>Na^{+}>PO3- 4 > K^{+}>NO- 3 > Mg^{2+}>F^{-} > Cl^{-}. As can be seen that, SO2- 4, NH+ 4, Ca^{2+} and Na^{+} are the four most abundant ions, while NO- 3 is less significant. The present results show that the concentration of Ca^{2+} is significant, originating probably from the incineration of limestone in the raw materials. The relatively large content of SO2- 4 might be due to the high temperature inside the furnace (Seinfeld et al., 1998), which will facilitate the oxidation of SO_2 into S(VI) during the clinker calcination process, and lead to the formation of sulfate. The concentrations of SO2- 4and K^{+} increase with the increasing addition of MSS, indicating that the co-processing of MSS can effectively promote the emission of vitriolic and potassic PM. Previous studies reported that the incineration of biomass could increase the concentration of SO2- 4 (Rastogi et al., 2014), and MSS is similar, containing biomass-like species. For K^{+}, as it is also an important inorganic component in biomass burning emissions and is often used as a tracer for the biomass combustion, its high content in the PM points to the significant influence of MSS incineration.

The correlations between the molar equivalent of cations and anions are shown in Fig. S3. The molar ratio of measured anions to cations is much larger than 1 (slope: 1.903), indicating a large excess of anions. If carbonate is considered, which is possibly exiting in the PM but not measured here, the excess of anion would even larger (Xu et al., 2013). This result strongly indicates that the PM emitted from cement production is highly acidic. The secondary inorganic aerosol (SIA) components - NO- 3, SO2- 4and NH+ 4, relevant to corresponding precursor gases of NO_x, SO_2 and NH_3, are the major components that affect the particle acidity. The molar

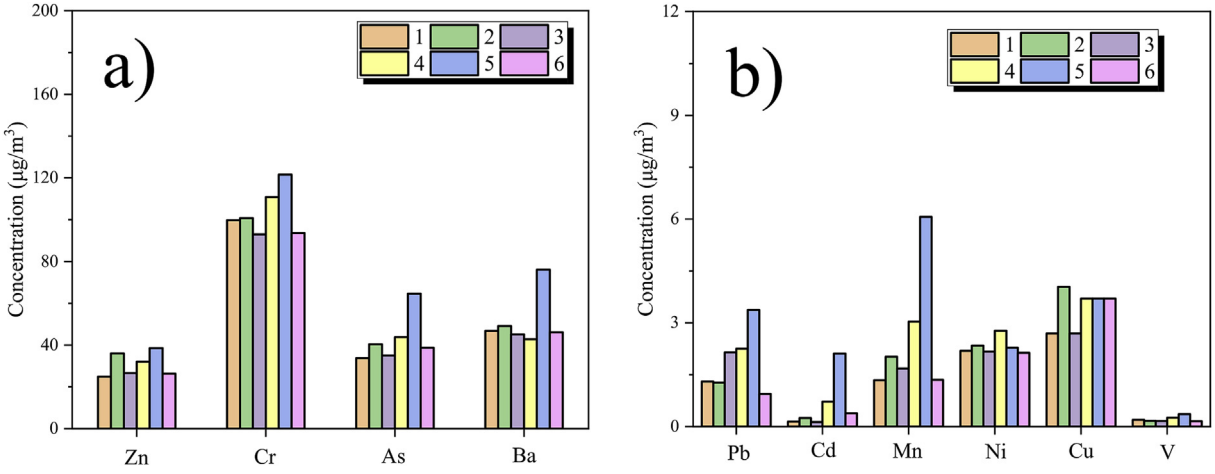

Fig. 2. The concentration heavy metals in PM (number 1–6 stand for the sample names as shown in Table S1).

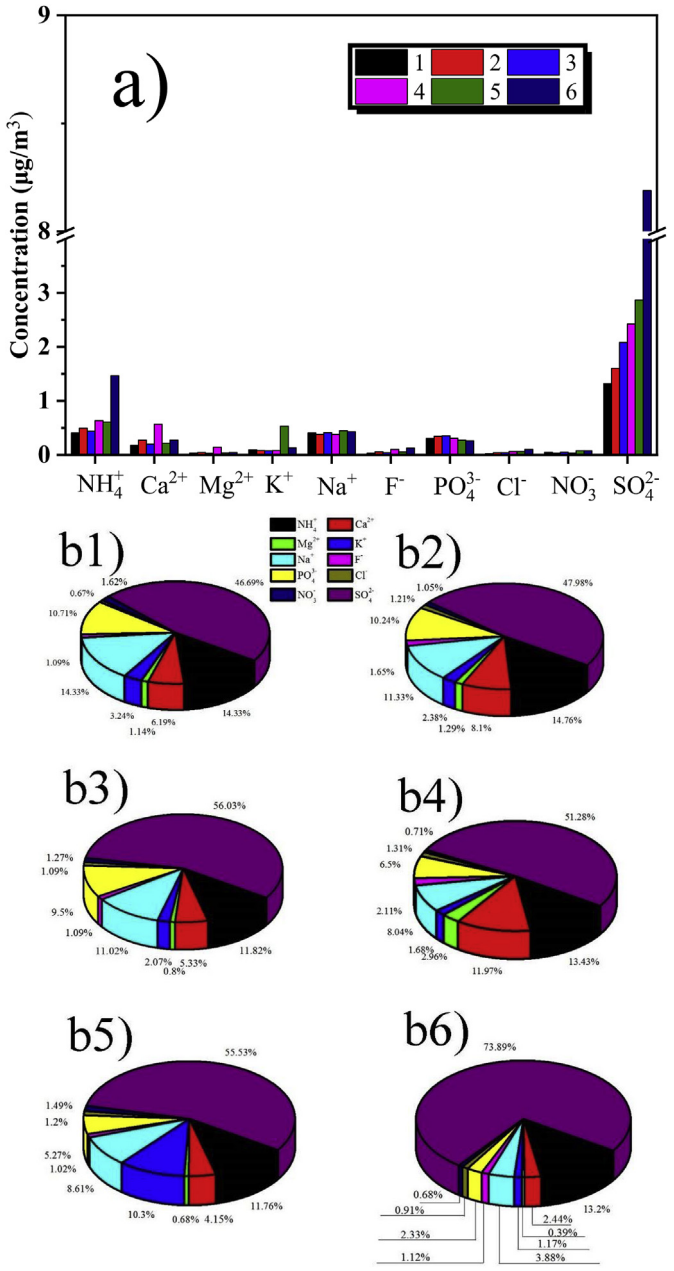

Fig. 3. a) Concentration of water-soluble ions in particulate matter, b) Percentage of water-soluble ions to the total ions; b1) Sample 1; b2) Sample 2; b3) Sample 3; b4) Sample 4; b5) Sample 5; b6) Sample 6.

ratio of [NH+ 4] to [SO2− 4] is an indicator used to estimate the neutralization of all the three SIA species. Generally, sulfate is considered to be fully neutralized at [NH+ 4]/[SO2− 4] ≥ 2 as $(NH_4)_2SO_4$ is formed. The values of [NH+ 4]/[SO2- 4] for samples 1 to 6 are 1.63, 1.64, 1.12, 1.40, 1.13 and 0.95, respectively. All values are significantly smaller than 2, indicating that sulphuric acid cannot be neutralized by the available ammonia in the air. If nitrate is added to the neutralization reactions, the equivalent molar ratios (microequivalents) of measured NH+ 4to the sum of NO− 3and SO2− 4 are also much less than 1, as shown in **Fig. S4**. This result clearly shows a large deficiency of ammonia, and the PM is in excess of sulfate and nitrate. The mass fraction of SO2- 4 also increased sharply with the increase of MSS amounts, indicating that the PM becomes even more acidic when more MSS is processed. Such highly acidic PM might bring significant impacts on the air quality in the vicinity of the production plant.

3.3. Characterization of WSOM in PM

The mass spectra determined by the by SP-AMS for the WSOM in PM are shown in Fig. 4. It should be noted that SP-AMS cannot accurately quantify metal species, such as Na^+, K^+ and Mg^{2+}. The SP-AMS can only determine the non-refractory species, and there are also possible loss of NO- 3, SO2- 4 and Cl^- during nebulization of the liquid extract. The inorganic components determined by the SP-AMS are different from those measured by IC. The SP-AMS results reveal that the mass fractions of organics in the PM can increase with the increasing addition of MSS, which can be attributed to the high content of volatile matter that MSS contains (Yang et al., 2016). This indicates that the addition of MSS in cement kiln can increase the WSOM content in the PM emitted.

The mass spectra of WSOM are dominated by oxygen-containing ion fragments of $C_xH_yO_1^+$ and $C_xH_yO_2^+$. Typically, the PM directly emitted from the simulated cement production process is primary and fresh particles, which are expected to be less oxygenated and have more chemically reduced hydrocarbon species, similar to the vehicular particles (Zhou, 2015). The observed high contents of oxygenated ions here are likely because we only measured the water-soluble portion of organics. Previous studies demonstrate that a large portion of primary particles are water-insoluble. On the contrary, the oxygenated organics, on the contrary, have larger water solubility (Lu et al., 2017). It is suggested that, in future study, online analyses of the emitted PM should be conducted rather than only on the water extracts, to elucidate the chemical properties of PM better. In the WSOM spectra, the prominent peaks of $C_2H_3^+$, $C_3H_3^+$, $C_3H_5^+$, $C_3H_7^+$ and $C_4H_7^+$ have relatively large intensities. These organic moieties are produced from the hydrocarbon-related species, which are clearly relevant to the MSS combustion. The mass spectra also show that the ions with m/z values larger than 100 amu are also dominated by $C_xH + y$ ions, which are likely to be fragments of long-chain alkanes (Wang et al., 2016b) and can be related to the MSS combustion. Some organic nitrogen-containing species, such as CN^+ and CHN^+, are attributed to biomass burning (Ge et al., 2011); the existence of these two ions in the mass spectrum also indicates the influence of MSS combustion. It can be seen from Fig. 4 that, the content of $C_xH_yN + p$ in WSOM increases with the increasing MSS amounts. This outcome also confirms that the addition of MSS can enhance the formation of organic nitrogen-containing species in PM.

3.4. Mixing states of particles in PM

On the basis of the different elemental composites and morphologies, nine kinds of particles: Ca-rich, S-rich, Na-rich, K-rich, metal, fly ash, organic, mineral and soot particles can be identified, as shown in Fig. 5. The classified method has been illustrated by previous studies in detail (Li et al., 2016), and most particles are found to mix with other types of particles (Fig. 6).

K-rich particles are irregularly shaped, and abundant of K and S (Fig. 5a), which is mainly from the biomass combustion (Li et al., 2010), relating to MSS incineration in the present context. Na-rich particles are cubic-shaped (Fig. 5b) and their size in this study are smaller than those from the natural sources (Li et al., 2015a,b), suggesting that they are apparently from the anthropogenic sources (wastes or coal incineration). The elemental mapping of K-rich and Na-rich particles are shown in Fig. 7, indicating that the Na-rich and K-rich particles are mainly in the forms of Na_2SO_4 and K_2SO_4. Due to the high chlorine content in the MSS, it is surmised that the Na-rich and K-rich particles should possess a high amount of NaCl

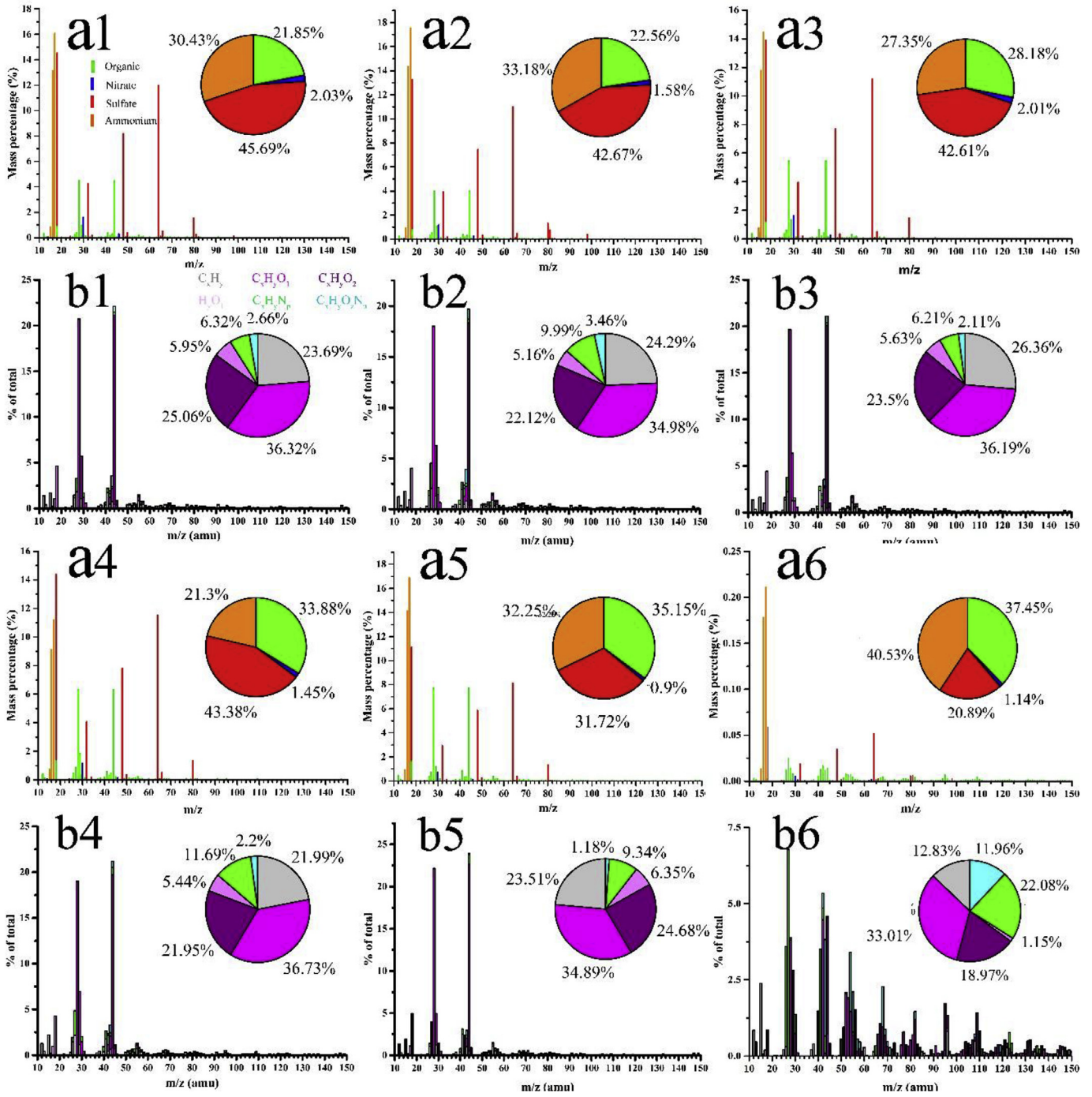

Fig. 4. (a) The SP-AMS determined averaged mass spectrum of water-soluble species in PM, and (b) the average mass spectrum of WSOM classified by six ion categories. The numbers in the figure represent the corresponding sample name, e.g., a1) represents the SP-AMS mass spectrum of Sample 1; b1) is the average mass spectrum of organics for Sample 1. The inset pie charts show the relative contributions of different components to the water-soluble PM, and the six ion categories to the total organics.

and KCl. The most likely reason could be the heterogeneous reactions among the NaCl, KCl and SO_2, which can quickly generate Na_2SO_4 and K_2SO_4 (Li et al., 2016), leading to the high content of SO2− 4in the PM, in accordance with the inorganic ionic analysis results. S-rich particles contain O, S and minor amounts of K. These particles appear as bubble-shaped because they are extremely beam sensitive. Most of the S-rich particles are found to mix with other particles, such as organic, metals and mineral particles. Spherical fly ash particles are composed by Si and O (Fig. 5d), and they are commonly produced by the aerosols from coal combustion (Li and Shao, 2009). Ca-rich particles appear as cube-shaped (Fig. 5e), mainly composed of Ca, C and O, which might come from the incineration of limestone in cement raw meal. Metal particles contain multiple heavy metals (Fig. 5f) and those particles are always embedded in the sulphates, which are likely to have been released from the combustion of coal and MSS. Mineral particles display as irregular shapes and are mainly composed by Si and O. These mineral particles are stable in the electron beam and, are found to mix with the Na–K-rich particles. Soot particle appears as aggregates of carbon-bearing spheres and, its morphology is

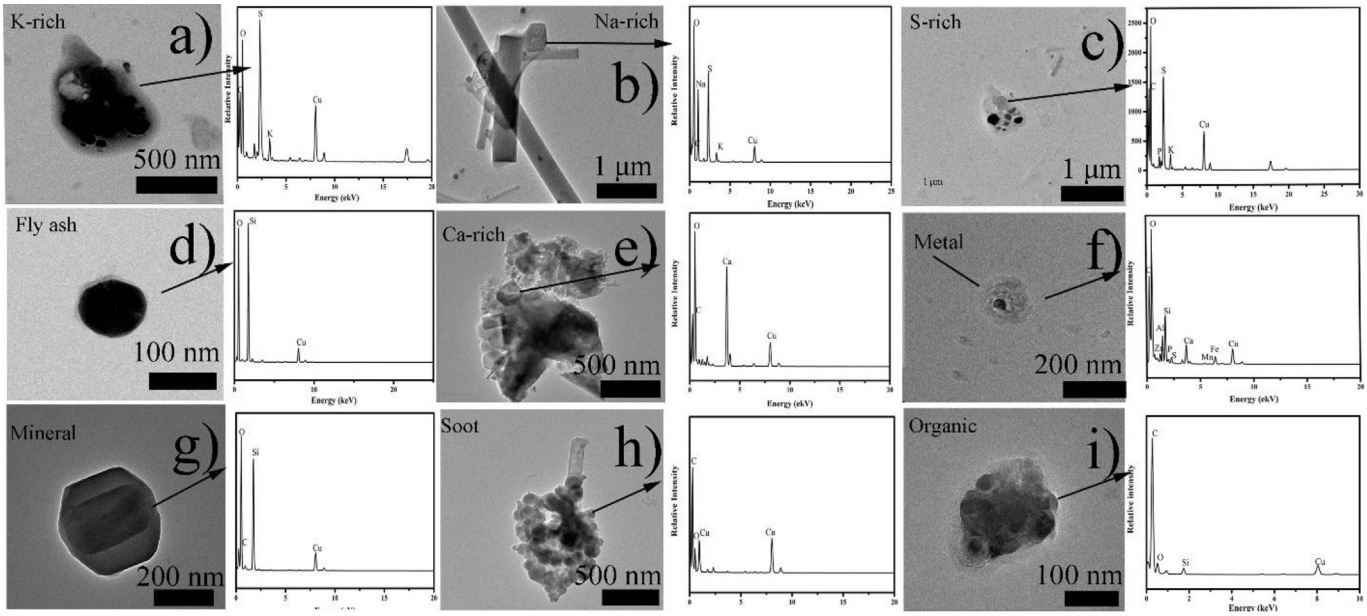

Fig. 5. TEM images of different types of particles: (a) K-rich particle, (b) Na-rich particle, (c) S-rich particle, (d) Fly ash particle, (e) Ca-rich particle, (f) Metal contained particle, (g) Mineral particles, (h) Soot particles, (i) Organic particle.

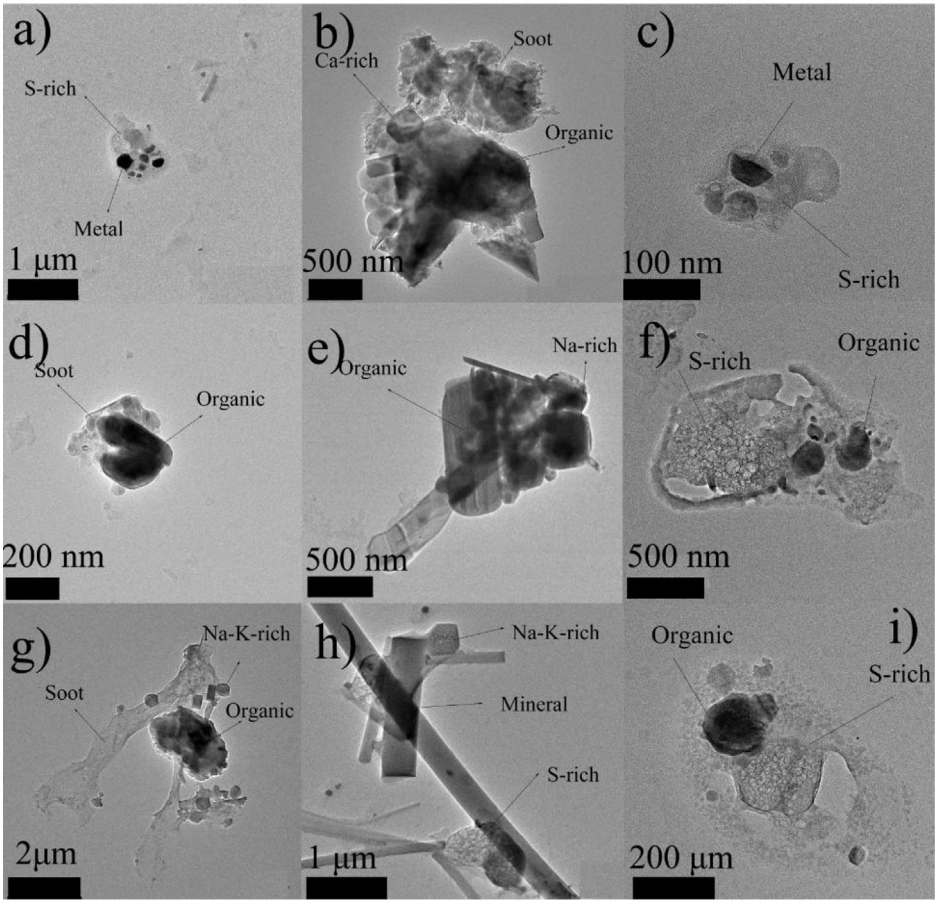

Fig. 6. TEM images of the representative mixed particles: (a) S-rich and metal particles, (b) Ca-rich, organic and soot particles, (c) S-rich and metal particles, (d) Soot and organic particle, (e) Organic and Na-rich particle, (f) Organic and S-rich particle, (g) Na–K-rich, soot and organic particle, (h) Na–K-rich, mineral and S-rich particle, (f) Organic and S-rich particle.

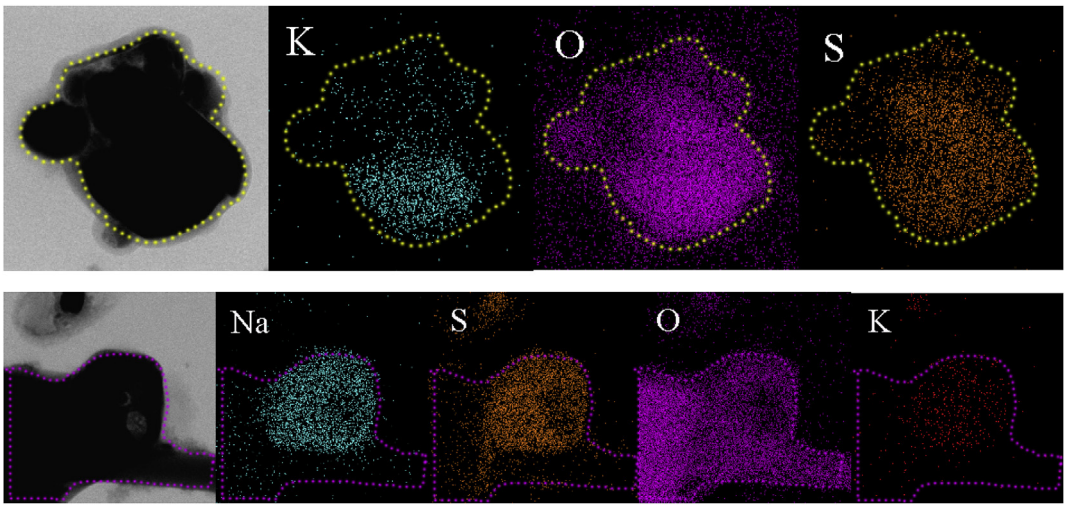

Fig. 7. The elemental mapping of K-rich and Na-rich particle.

different from that of the organic particle, although they have similar elemental compositions. These particles are mainly from the incomplete combustion of coal and MSS and tend to mix with organic and Na–K-rich particles. Organic particles display irregular shapes (Fig. 5i), mainly containing C and O, and spherical particles probably comprise of the tar balls from MSS burning (Chakrabarty et al., 2006). According to the TEM observation, most organic particles are mixed with soot and S-rich particles. Single particle analysis can also demonstrate the mixing states of the particles (Fig. 6). For instance, organic and heavy metals particles can be found as inclusions coated with sulfate or adhere onto the sulphates. Soot, mineral and organic particles are frequently observed to adhere onto each other. Those mixing states observations could help to understand the formation processes of PM and their environmental impacts. This is further discussed in the next section.

3.5. Possible mechanism of PM formation

Based on the TEM observations, a framework for the formation of different mixing structures can be proposed (Fig. 8). Most of the particles tend to internally mix or externally mix with other particles (Fig. 7). These mixed particles are postulated to be formed through two steps.

In the first step, PM with different compositions can be released through multiple chemical processes, which have been already proved by the previous studies. Sulfate (sulfur-rich) particles can be generated through the gas phase oxidation of SO_2 (Mao et al., 2011). The organic compounds in the raw materials and fuel can be directly emitted in the form of PM, and some other organics can be oxidized into low-volatile organics, which may condense on pre-existing particles or form new organic particles (Li et al., 2016).

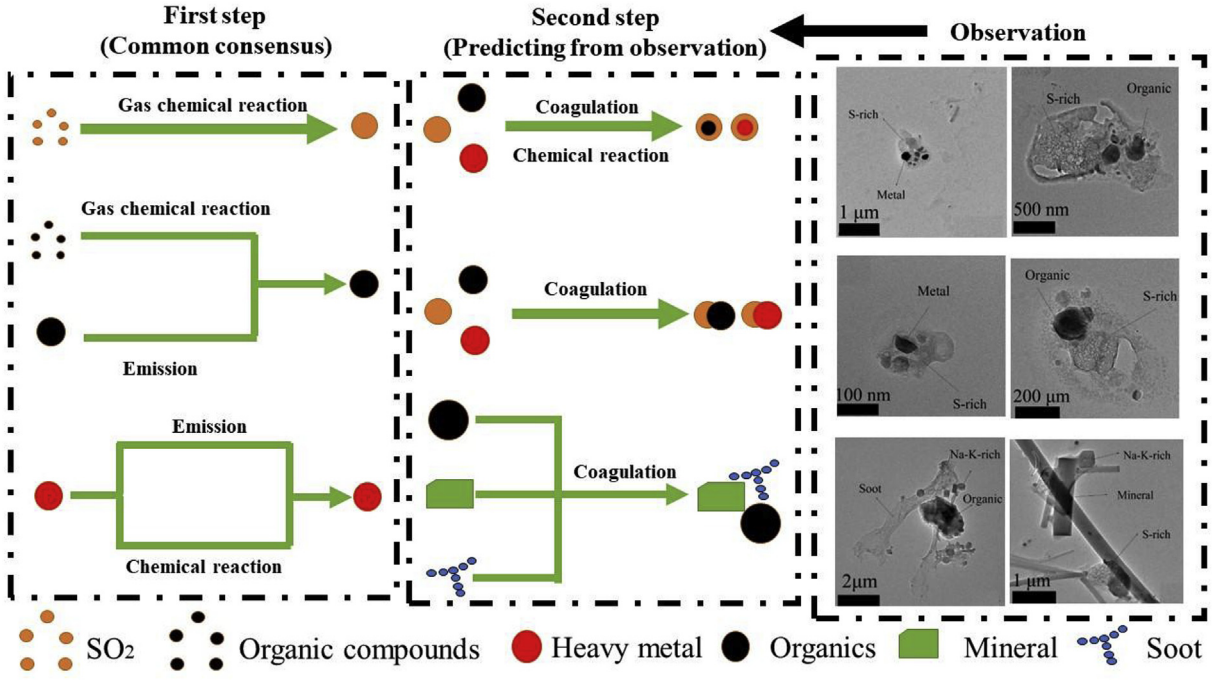

Fig. 8. Schematic of mixing structures of different particle types.

The metal-containing particles (Ca-rich, Na-rich, K-rich, or other heavy metal-rich) can be directly emitted into the air due to incineration of raw materials, such particles can also coagulate and form other types of metal-containing particles. Soot particles are known to be generated through incomplete combustion of MSS and coal (Yang et al., 2018). In the second stage, the PM with various mixing structures are formed. Based on the corresponding TEM observations, formations of such mixed PM were mainly due to chemical reactions, physical coagulations or their combined effects. Correspondingly, TEM evidences for such mechanisms are provided. As shown in the right panel of Fig. 8, first, mixed structures of sulfate/metal particles and sulfate/organic particles are observed. Note since sulfate is secondarily formed, this observation on one hand, indicates possible heterogeneous chemical formation of sulfate on metal or organic particles, and on the other hand, more metal-containing or organic particles may directly coagulate, adhere onto the sulfate particles. Secondly, soot-metal-organic mixed particles, and metal-mineral-sulfate particles, etc., are also observed. Particularly, since soot and mineral particles are primary, their presences in mixed PM indicate formation of such particles are mainly through coagulation. As different types of particles have different sizes and morphologies, the combined effect of coagulation and chemical reactions thus would lead to a wide variety of mixed PM as we observed in Fig. 6 during the cement kiln production process. It is known that these mixing states can alter the hygroscopicity and optics of the PM (Ramanathan and Carmichael, 2017), posing adverse effects on the environment in the vicinity of the cement plant. For example, the hydrophobic particles (fly ash, organics and soot) with the sulfate coating can become hygroscopic, which can grow bigger through absorption of water along with the increase of relative humidity. Such particles can to some extent impact the atmospheric light scattering and absorption, which can alter the climate forcing effect. As can be seen, the soot particles adhered onto the surface of sulfate particles were dominant in this study, which might decrease light absorption by 30% compared to that corresponding to that of within the sulfate particles (Li et al., 2015a,b) Metal particles inside the sulfate particles might involve in multiphase metal-catalysed chemical reactions during their long-range transport and further influence human health (Li et al., 2013). As the MSS contains much higher contents of heavy metals than the regular fuel and raw materials, the co-processing of MSS in a cement kiln can facilitate the emission of such metal-containing particles, which might pose a threat to the inhabitants' health in the vicinity of cement plant. The secondary species are found to be a dominant component of fine PM (Huang et al., 2014). The mass proportions of SO2- 4and secondary organics in PM increase with the addition of MSS, which indicates that the co-processing of wastes in cement kiln might contribute to the PM pollution and haze formation.

It should be pointed out that, due to the limitation of experimental equipment, the rotary kiln, used in cement manufacturing cannot be simulated in the present laboratory. In the present experiments, it is suggested that the PM can be formed in two ways:

1 PM can be directly emitted from the combustion of fuel;
2 Volatile species can be released during the combustion of fuel and then be transformed to PM. This latter process can be complete in a short time. The PM can subsequently react with raw materials and be released out, which is similar with that in the cement kiln. Although some experimental conditions in the laboratory-scale study are different from those in the real production process. For example, coal is not mixed with raw materials in the real cement kiln. The present results can be of significance in understanding how the MSS affects the formation and chemical properties of PM. Our investigation on addition of coal is also valuable for future possible technical development. Future work will explore the interactions and co-founding effects of the chemical species of wastes, the properties of emitted PM and operating conditions in the rotary kiln condition by establishing a miniature rotary kiln in laboratory.

4. Conclusion and implications

The co-processing of MSS to produce cement is a cleaner production process for the waste reduction, but the secondary pollution issue, namely the emitted PM that is likely harmful to human health and local air quality has been overlooked in some extent. The present investigation therefore focused on the chemical compositions, morphologies and formation mechanism of PM released from a laboratory-scale simulated cement kiln co-processing wastes. Composition of raw materials, experimental conditions are based on real production process, our findings can reflect the real processes despite some differences might exist. We found that EFs of heavy metals, and the mass proportions of sulfate and organics in PM increased with increasing addition of MSS. These results indicate that the co-processing of MSS in cement kilns can promote the enrichment of heavy metals, secondary inorganic species and organics in PM, likely causing more serious effects on the air quality and human health than the background PM. Particles emitted are always present as the mixture of different types of particles and their formation mechanisms are also proposed in the present study. These findings suggest that although the technology of co-combustion wastes in cement kiln offer multiple advantages, it may also pose a threat to the regional environment and human health at the same time due to the emitted PM from such process.

Of course, our findings here are based on a simulated industrial process, future studies in large-scale processes are necessary to achieve a more comprehensive environmental and sustainability assessment of the technology. Nevertheless, our results here call attentions to the secondary environmental pollution issue (PM pollution) from a promising clean process of MSS utilization, and provide clues to make a stricter emission standard when such a technology is implemented, and also improved gas cleaning techniques to tackle the increased emissions. This work is therefore beneficial to the goal of cleaner production, environmental protection and sustainable development.

Acknowledgements

This study was supported by National Natural Science Foundation of China (51772141). This work was also supported financially by Research Funding supported by Shenzhen Science and Technology Innovation Committee (JCYJ20170412154335393, KQTD2016022619584022). Additional support was provided by Guangdong Provincial Key Laboratory of Soil and Groundwater Pollution Control (Grant No. 2017B030301012).

Appendix A. Supplementary data

Supplementary data to this article can be found online at https://doi.org/10.1016/j.jclepro.2019.06.280.

References

Aiken, A.C., Decarlo, P.F., Kroll, J.H., Worsnop, D.R., Huffman, J.A., Docherty, K.S., Ulbrich, I.M., Mohr, C., Kimmel, J.R., Sueper, D., 2008. O/C and OM/OC ratios of primary, secondary, and ambient organic aerosols with high-resolution time-of-flight aerosol mass spectrometry. Environ. Sci. Technol. 42 (12), 4478–4485.
Asamany, E.A., Gibson, M.D., Pegg, M.J., 2017. Evaluating the potential of waste plastics as fuel in cement kilns using bench-scale emissions analysis. Fuel 193, 178–186.

Becidan, M., Sørum, L., Lindberg, D., 2010. Impact of municipal solid waste (MSW) quality on the behavior of alkali metals and trace elements during combustion: a thermodynamic equilibrium analysis. J. Stud. Alcohol Drugs 74 (4), 514–520.
Chakrabarty, R.K., Moosmüller, H., Garro, M.A., Arnott, W.P., Walker, J., Susott, R.A., Babbitt, R.E., Wold, C.E., Lincoln, E.N., Hao, W.M., 2006. Emissions from the laboratory combustion of wildland fuels: particle morphology and size. J. Geophys. Res. Atmos. 111 (D7), 1–16.
Dongarrà, G., Manno, E., Varrica, D., Vultaggio, M., 2007. Mass levels, crustal component and trace elements in PM in Palermo. Italy Atmos. Environ. 41 (36), 7977–7986.
Folgueras, M.B., Dıaz, R.M.A., Xiberta, J., 2004. Sulphur retention during co-combustion of coal and sewage sludge. Fuel 83 (10), 1315–1322.
Gao, J., Tian, H., Cheng, K., Lu, L., Wang, Y., Wu, Y., Zhu, C., Liu, K., Zhou, J., Liu, X., 2014. Seasonal and spatial variation of trace elements in multi-size airborne particulate matters of Beijing, China: mass concentration, enrichment characteristics, source apportionment, chemical speciation and bioavailability. Atmos. Environ. 99, 257–265.
Ge, X., Li, L., Chen, Y., Chen, H., Wu, D., Wang, J., Xie, X., Ge, S., Ye, Z., Xu, J., 2017. Aerosol characteristics and sources in Yangzhou, China resolved by offline aerosol mass spectrometry and other techniques. Environ. Pollut. 225, 74–85.
Ge, X., Shaw, S.L., Zhang, Q., 2014. Toward understanding amines and their degradation products from postcombustion CO_2 capture processes with aerosol mass spectrometry. Environ. Sci. Technol. 48 (9), 5066–5075.
Ge, X., Wexler, A.S., Clegg, S.L., 2011. Atmospheric amines – Part I. A review. Atmos. Environ. 45 (3), 524–546.
Huang, R.J., Zhang, Y., Bozzetti, C., Ho, K.F., Cao, J.J., Han, Y., Daellenbach, K.R., Slowik, J.G., Platt, S.M., Canonaco, F., 2014. High secondary aerosol contribution to particulate pollution during haze events in China. Nature 514 (7521), 218–222.
Jeschar, R., Jennes, R., Kremer, H., Kellerhoff, T., 1999. Reducing NO_x and CO emissions by burning plastics in the calciner of a rotary cement kiln plant. ZKG Int. 52 (10), 534–549.
Jin, J., Wang, M., Cao, Y., Wu, S., Liang, P., Li, Y., Zhang, J., Zhang, J., Wong, M.H., Shan, S., 2017. Cumulative effects of bamboo sawdust addition on pyrolysis of sewage sludge: biochar properties and environmental risk from metals. Bioresour. Technol. 228, 218–226.
Jin, R., Zhan, J., Liu, G., Zhao, Y., Zheng, M., 2016. Variations and factors that influence the formation of polychlorinated naphthalenes in cement kilns co-processing solid waste. J. Hazard Mater. 315, 117–125.
Li, C., 2013. Cluster analysis of the chlorine content in the cement kiln alternative fuels. Environ. Eng. 31, 570–572.
Li, W.J., Chen, S.R., Xu, Y.S., Guo, X.C., Sun, Y.L., Yang, X.Y., Wang, Z.F., Zhao, X.D., Chen, J.M., Wang, W.X., 2015a. Mixing state and sources of submicron regional background aerosols in the northern Qinghai–Tibet Plateau and the influence of biomass burning. Atmos. Chem. Phys. 15 (23), 13365–13376, 2015-12-02) 15(23).
Li, W., Shao, L., 2009. Transmission electron microscopy study of aerosol particles from the brown hazes in northern China. J. Geophys. Res. Atmos. 114 (D9), 1–10.
Li, W., Shao, L., Zhang, D., Ro, C.U., Hu, M., Bi, X., Geng, H., Matsuki, A., Niu, H., Chen, J., 2016. A review of single aerosol particle studies in the atmosphere of East Asia: morphology, mixing state, source, and heterogeneous reactions. J. Clean. Prod. 112, 1330–1349.
Li, W., Wang, T., Zhou, S., Lee, S.C., Huang, Y., Gao, Y., Wang, W., 2013. Microscopic observation of metal-containing particles from Chinese continental outflow observed from a non-industrial site. Environ. Sci. Technol. 47 (16), 9124–9131.
Li, W.J., Chen, S.R., Xu, Y.S., Guo, X.C., Sun, Y.L., Yang, X.Y., Wang, Z.F., Zhao, X.D., Chen, J.M., Wang, W.X., 2015b. Mixing state and sources of submicron regional background aerosols in the northern Qinghai-Tibet Plateau and the influence of biomass burning. Atmos. Chem. Phys. 15 (23), 13365–13376.
Li, W.J., Shao, L.Y., Buseck, P.R., 2010. Haze types in Beijing and the influence of agricultural biomass burning. Atmos. Chem. Phys. 10 (17), 8119–8130.
Lu, X., Guo, H., Weber, R.J., Ng, N.L., 2017. Chemical characterization of water soluble organic aerosol in contrasting rural and urban environments in the southeastern United States. Environ. Sci. Technol. 51 (1), 78–88.
Mao, H.Y., Tian, G., Huang, Y.H., Li, G., Song, G.W., 2011. Mass size distributions and existing forms of sulfate and nitrate at atmospheric environment in Beijing. Environ. Sci. 32 (5), 1237–1241.
Ramanathan, V., Carmichael, G., 2017. Global and regional climate changes due to black carbon. Nat. Geosci. 36 (1), 335–358.
Rastogi, N., Singh, A., Singh, D., Sarin, M.M., 2014. Chemical characteristics of $PM_{2.5}$ at a source region of biomass burning emissions: evidence for secondary aerosol formation. Environ. Pollut. 184 (1), 563–569.
Schuhmacher, M., Nadal, M., Domingo, J.L., 2009. Environmental monitoring of PCDD/Fs and metals in the vicinity of a cement plant after using sewage sludge as a secondary fuel. Chemosphere 74 (11), 1502–1508.
Seinfeld, J.H., Pandis, S.N., Seinfeld, J.H., Pandis, S.N., 1998. Atmospheric chemistry and physics: from air pollution to climate change. Environment 40 (7), 26-26.
Sun, Y.L., Wang, Z.F., Du, W., Zhang, Q., Wang, Q.Q., Fu, P.Q., Pan, X.L., Li, J., Jayne, J., Worsnop, D.R., 2015. Long-term real-time measurements of aerosol particle composition in Beijing, China: seasonal variations, meteorological effects, and source analysis. Atmos. Chem. Phys. 15 (17), 10149–10165.
Wang, G., Zhang, R., Gomez, M.E., Yang, L., Zamora, M.L., Hu, M., Lin, Y., Peng, J., Guo, S., Meng, J., 2016a. Persistent sulfate formation from London fog to Chinese haze. Proc. Natl. Acad. Ofences U.S.A. 113 (48), 13630–13635.
Wang, N.F., Chen, Y., Hao, Q.J., Wang, H.B., Yang, F.M., Zhao, Q., Bo, Y., He, K.B., Yao, Y.G., 2016b. Seasonal variation and source analysis of the water-soluble inorganic ions in fine particulate matter in Suzhou. Environ. Sci. 37 (12), 4482–4489.
Xiao, B., Dai, Q., Yu, X., Yu, P., Zhai, S., Liu, R., Guo, X., Liu, J., Chen, H., 2017. Effects of sludge thermal-alkaline pretreatment on cationic red X-GRL adsorption onto pyrolysis biochar of sewage sludge. J. Hazard Mater. 343, 347–355.
Xu, J., Zhang, Q., Li, X., Ge, X., Xiao, C., Ren, J., Qin, D., 2013. Dissolved organic matter and inorganic ions in a central Himalayan glacier insights into chemical composition and atmospheric sources. Environ. Sci. Technol. 47 (12), 6181–6188.
Yang, Z., Tang, S., Zhang, Z., Liu, C., Ge, X., 2018. Characterization of PM_{10} surrounding a cement plant with integrated facilities for co-processing of hazardous wastes. J. Clean. Prod. 186, 831–839.
Yang, Z., Zhang, Y., Liu, L., Wang, X., Zhang, Z., 2016. Environmental investigation on co-combustion of sewage sludge and coal gangue: SO_2 , NO_x and trace elements emissions. Waste Manag. 50, 213–221.
Zhao, Y.B., Gao, P.P., Yang, W.D., Ni, H.G., 2018. Vehicle exhaust: an overstated cause of haze in China. Sci. Total Environ. 612, 490–491.
Zhou, H.B., Ma, C., Gao, D., Chen, T.B., Zheng, G.D., Chen, J., Pan, T.H., 2014. Application of a recyclable plastic bulking agent for sewage sludge composting. Bioresour. Technol. 152 (152), 329–336.
Zhou, S., 2015. Organic PM emissions from vehicles: composition, O/C ratio, and dependence on PM concentration. Aerosol Sci. Technol. 49 (2), 86–97.